



## Review

## Structural and material approaches to bone tissue engineering in powder-based three-dimensional printing

A. Butscher<sup>a,b,\*</sup>, M. Bohner<sup>a</sup>, S. Hofmann<sup>b</sup>, L. Gauckler<sup>c</sup>, R. Müller<sup>b</sup><sup>a</sup>RMS Foundation, Bischmattstrasse 12, CH-2544 Bettlach, Switzerland<sup>b</sup>Institute for Biomechanics, ETH Zurich, Wolfgang-Pauli-Strasse 10, CH-8093 Zurich, Switzerland<sup>c</sup>Institute for Nonmetallic Inorganic Materials, ETH Zurich, Wolfgang-Pauli-Strasse 10, CH-8093 Zurich, Switzerland

## ARTICLE INFO

## Article history:

Received 1 July 2010

Received in revised form 9 September 2010

Accepted 28 September 2010

Available online 16 October 2010

## Keywords:

Tissue engineering

Scaffold

Bone substitute

Calcium phosphate

Solid free-form fabrication

## ABSTRACT

This article reviews the current state of knowledge concerning the use of powder-based three-dimensional printing (3DP) for the synthesis of bone tissue engineering scaffolds. 3DP is a solid free-form fabrication (SFF) technique building up complex open porous 3D structures layer by layer (a bottom-up approach). In contrast to traditional fabrication techniques generally subtracting material step by step (a top-down approach), SFF approaches allow nearly unlimited designs and a large variety of materials to be used for scaffold engineering. Today's state of the art materials, as well as the mechanical and structural requirements for bone scaffolds, are summarized and discussed in relation to the technical feasibility of their use in 3DP. Advances in the field of 3DP are presented and compared with other SFF methods. Existing strategies on material and design control of scaffolds are reviewed. Finally, the possibilities and limiting factors are addressed and potential strategies to improve 3DP for scaffold engineering are proposed.

© 2010 Acta Materialia Inc. Published by Elsevier Ltd. All rights reserved.

## 1. Introduction

Broad awareness of the term “tissue engineering” started with the publication of a paper by Langer and Vacanti in 1993 [1]. This review paper stated a now commonly used definition of tissue engineering as “an interdisciplinary field that applies the principles of engineering and life sciences toward the development of biological substitutes that restore, maintain or improve tissue function or a whole organ”.

Whereas in the late 1990s tissue engineering envisioned the replacement of whole tissues or even organs, today a tendency towards preventive medicine can be noticed. Therefore, it is speculated that the greatest impact of tissue engineering in the next decade might be in vitro physiological models to study disease pathogenesis, thus allowing the development of drugs that can eliminate or reduce the need for tissue replacement [2].

The standard approach in bone tissue engineering is to seed and grow cells on scaffolds in vitro. Typical scaffolds are three-dimensional (3D) porous structures trying to temporarily mimic the natural extracellular matrix of bone. Porous structures seem to play a significant role in nature, nicely described in the following statement by Ashby [3]:

“When modern man builds large load bearing structures, he uses dense solids: steel, concrete, glass. When nature does the same, she generally uses cellular materials: cork, wood, coral. There must be good reason for it.”

Following this principle the “art of structure is where to put the holes” or the “art of scaffolding is where to put the holes, biofactors and cells” [4]. Scaffold design properties are a key factor in bone tissue engineering and represent more than just a passive component. Scaffold design will control cell and ultimately tissue growth by balancing mechanical function with drug delivery, as well as degradation of the scaffold adjusted to tissue regeneration [4].

Conventional manufacturing methods used in traditional engineering fields are top-down approaches, starting from simple, large solids and fabricating those into smaller complex products. Complex porous 3D structures are particularly demanding concerning design and often infeasible to produce by conventional approaches. Therefore, random processes such as foaming [5], salt leaching [6] and emulsification [7] are widespread, however, they can only partially fulfill the requirements set by tissue engineering approaches. One major drawback is the fact that porous scaffolds cannot be produced with full control of the geometrical parameters, such as pore size, pore interconnection size and porosity.

In contrast to top-down approaches, the bottom-up approach of solid free-form fabrication (SFF) typically starts with small building units (e.g. powders) that are arranged and piled up to eventually obtain the desired geometry. This iterative method is based on well-defined “sliced” 3D CAD models [8] resulting in nearly

\* Corresponding author at: RMS Foundation, Bischmattstrasse 12, CH-2544 Bettlach, Switzerland.

E-mail address: [andre.butscher@rms-foundation.ch](mailto:andre.butscher@rms-foundation.ch) (A. Butscher).

unlimited geometries by adding up small layers of the final structure. This is the crucial advantage of SFF making it suitable for the “art of scaffolding”.

Despite such a unique freedom in designing complex geometries, SFF approaches have rarely been used to manufacture commercial tissue engineering scaffolds (except, for example, Curasan AG, Germany and Integra Spine, USA). There are several reasons for this. For example, SFF approaches are still more expensive than presently used techniques. Also, the gain in biological performance due to an improvement of geometry has not been quantified. Furthermore, SFF approaches all face technical difficulties, such as limited accuracy, low mechanical properties and poor raw material availability. In recent years the prices for SFF machines have dropped and solutions have been proposed to limit or even solve the drawbacks of SFF, but many challenges remain.

There are several approaches in SFF. One of particular interest is so-called 3D printing (3DP). In 3DP the solid is created by the reaction of a liquid selectively sprayed onto a powder bed [9]. This liquid can either act as a binder or provoke a reaction that will bind the powder particles together, for example through a crystallization reaction. In the literature the term binder is used for both and so it will be in this manuscript. Once hardened, the layer is covered with a new powder layer, which is again locally bound to form a new solid layer. In other words, the powder bed acts not only as the reagent but also as physical support for the printed solid. This approach is very simple and versatile because many powdered materials can be used. In particular, this method can be adapted for the production of ceramic-based tissue engineering scaffolds [10].

Bone is able to self-regenerate, however, regeneration is limited to a distance of a few millimeters from healthy bone. So, to enhance bone regeneration bone defects must be filled with a porous spacer allowing the in-growth of blood vessel and bone but restricting soft tissue in-growth. In general, it is agreed that the porous network should consist of interconnected pores with a diameter in the range of 50–1000  $\mu\text{m}$  [7]. Since millions of bone defects must be healed each year, SFF techniques, and in particular 3DP, are of great interest for the manufacture of bone scaffolds. Therefore, the aim of this manuscript is to review the use of SFF techniques, in particular 3DP, for manufacturing bone scaffolds.

For this purpose the manuscript is divided into four parts. In the first part some of the most relevant structural properties of bone and present knowledge in the field of scaffold design are summarized. In the second part common methods of SFF used for scaffold engineering are compared and 3DP is described in detail. The third part is devoted to the technical aspects of 3DP, with an emphasis on the raw materials (powders) and the physico-chemical properties of the scaffolds. Moreover, technical possibilities and limitations using 3DP in the field of tissue engineering are discussed and set in relation to the biological requirements. Finally, the fourth part gives an outlook of the field and a conclusion.

## 2. Bone and scaffold engineering

### 2.1. Structural properties of bone

Following the approach of scaffolding as a way of temporarily mimicking the extracellular matrix of bone, it is necessary to look at the chemical, mechanical and structural properties of bone.

Bone is a sophisticated composite on different hierarchical levels. From a structural perspective, bone tissue consists of two main parts, a compact shell called cortical bone (“compact”) and a porous core called spongiosa or trabecular bone (“trabecular” meaning “little beam” in Latin [11]). The combination of a dense shear stress-resisting shell and a cellular inner structure with a typical

relative density of between 0.05 and 0.3 [12] prevents buckling and results in a lightweight core analogous to a sandwich structure with excellent bending resistance. In contrast to most man-made sandwich cores, trabecular bone has an optimized structural anisotropy due to the trabecular orientation along the principal stress trajectories [13]. On a nanometer scale bone can be basically described as a composite between 70% calcium phosphate crystals and 20–30% collagen matrix with some water [14]. This geometrically complex combination of an elastic collagen matrix (elastic modulus  $E = 1\text{--}2\text{ GPa}$ , ultimate tensile strength  $UTS = 50\text{--}1000\text{ MPa}$ ) with a hard and brittle calcium phosphate mineral ( $E = 130\text{ GPa}$ ,  $UTS = 100\text{ MPa}$ ) [15] leads to high mechanical bulk properties with ductile and thus failure-tolerant characteristics. According to a literature review the compressive strengths of cortical and cancellous bone are in the ranges 100–230 and 2–12 MPa, whereas the Young’s moduli are in the ranges 7–30 and 0.5–0.005 GPa, respectively [15]. While macro mechanical parameters are well described in the scientific literature, the mechanical properties at the micro- (osteons, Haversian canals), submicron (lamellae) and nano-structural (collagen fibers) levels remain poorly understood [16] and are still a matter of extensive research [17].

### 2.2. Scaffold requirements

In light of the complexity of bone properties, the goal of an ideal synthetic scaffold needs to be broken down into small, achievable steps.

A first step is to find a biocompatible material that also has the mechanical properties needed for a scaffold. Fig. 1 highlights the extraordinary mechanical properties of bone in contrast to technical bulk materials used for medical purpose. In detail, Young’s modulus is plotted against fracture toughness, which is a measure of the resistance of a material to crack propagation. Fracture toughness  $K_{Ic}$  (mode I fracture means the crack plane is normal to the direction of tensile loading) has units of  $\text{MPa m}^{1/2}$ . The graph depicts the relation between the elasticity of a material and its toughness (brittle materials like ceramics typically have a low toughness value). It reveals that up to now no artificial bulk material is able to mimic bone and serve as an ideal material for scaffold engineering. Bone seems to be the perfect lightweight optimum between elasticity, strength and fracture toughness. Instead of using bulk materials, cellular materials open up promising approaches.

Provided the material complies with the requirement of the selected SFF method, a second step is to build up the complex 3D (e.g. cellular) structures by means of SFF using building units small enough to reach the required resolution. The ultimate step is to improve the mechanical properties by, for example, a bioinspired composite approach, which is a matter of present and future research [18].

According to Hutmacher et al. [19] a scaffold should have the following main characteristics: (i) be biocompatible and bioresorbable with a controllable degradation and resorption rate to match cell/tissue growth in vitro and/or in vivo; (ii) have a suitable surface chemistry for cell attachment, proliferation and differentiation; (iii) be three-dimensional and highly porous with an interconnected porous network for cell growth, flow transport of nutrients and metabolic waste; (iv) have mechanical properties to match those of the tissues at the site of implantation. Unfortunately, it is at present obscure how this is applied in practice and in particular if a material fulfilling these criteria would really perform better than existing materials. Furthermore, the distinction between the requirements for tissue engineering and bone graft substitution scaffolds is still far from clear. Nevertheless, there is a general consensus that 3D bone scaffolds should be highly open porous structures (>40–60%) to favor rapid diffusion or the flow of

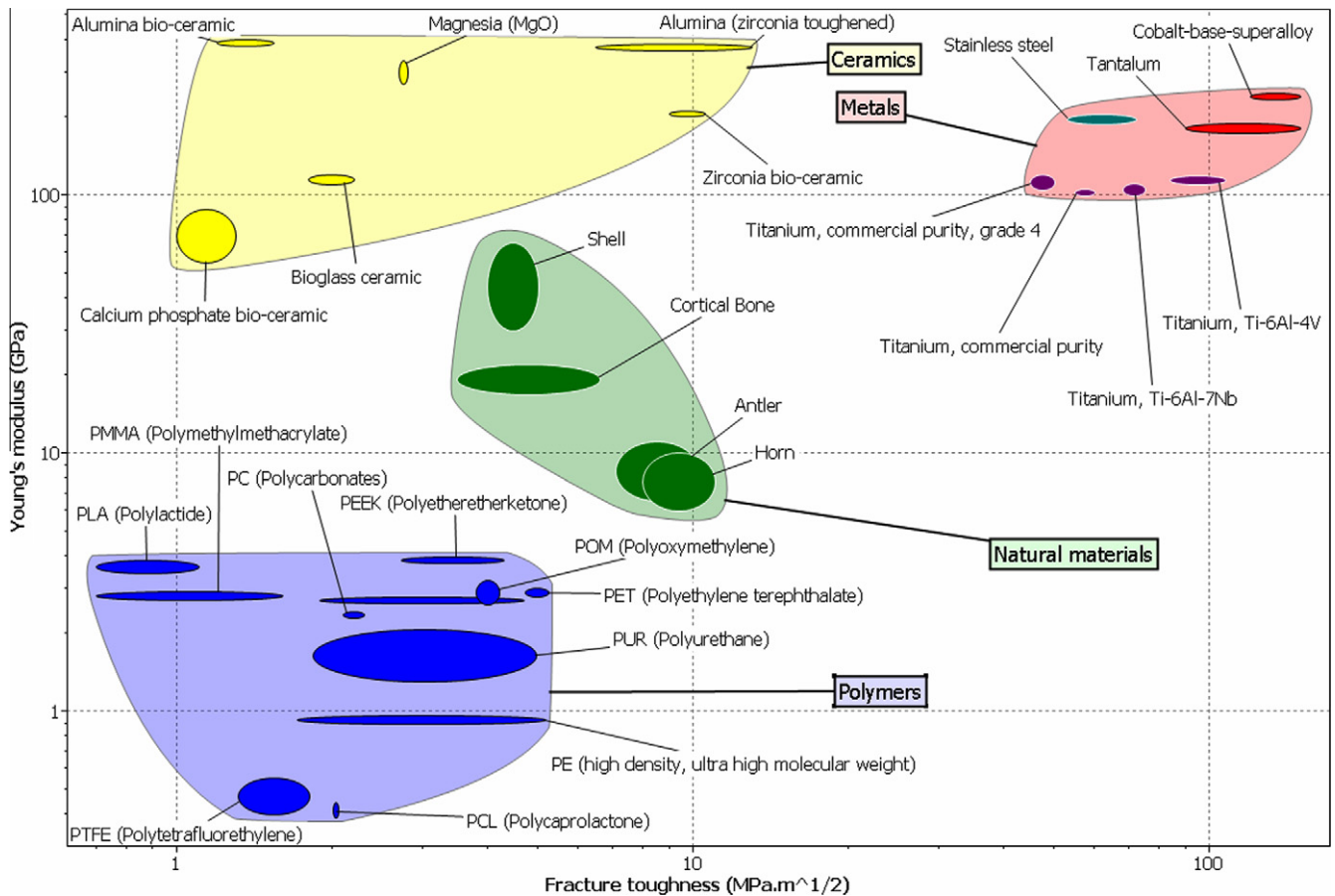


Fig. 1. Mechanical properties of natural materials in comparison with bulk materials for medical purpose (graph constructed with CES Selector 5.1.0).

cell nutrients and to allow cell migration [20]. Pore sizes necessary to achieve suitable porosities are suggested to be in the range 50–1000  $\mu\text{m}$  [7,21,22] for in vivo bone regeneration. In contrast, osteogenesis in vitro requires pore dimensions one order of magnitude lower than in vivo [22]. The size of the interconnections is still a matter of debate, with values of between 15 and 50  $\mu\text{m}$  [23,24]. Taking into account the assumptions and simplifications in all methods (gravimetry, mercury intrusion, liquid displacement, scanning electron microscopy (SEM) and computed tomography (CT)) [22] to determine pore parameters, an additional uncertainty arises. In this light it becomes obvious that instead of the “ideal” tissue engineering scaffold, different structures are needed for various applications.

### 2.3. Scaffold engineering

Scaffold engineering is always a trade-off between the biological requirements and technical feasibility. This paragraph focuses on the technical possibilities and limitations. Table 1 gives a short overview of the most commonly used SFF techniques used in the field of scaffold engineering. More details can be found in general reviews [4,25]. Table 1 reveals the key advantages of 3DP, such as a wide range of materials and simplicity when compared with other SFF methods.

The term SFF is also often referred to as rapid prototyping (RP). However this term is misleading in two aspects. Firstly, this process can be slow compared with conventional production methods. The focus is not on speed but on freedom in terms of geometry. Secondly, the term prototyping implies a limited application for pilot series. Therefore SFF instead of RP is used in this paper.

### 3. Powder-based three-dimensional printing (3DP)

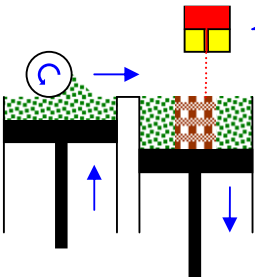
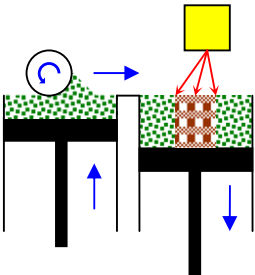
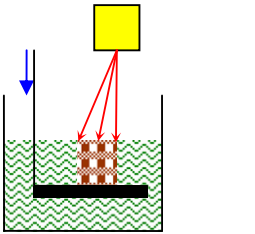
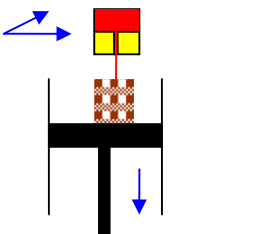
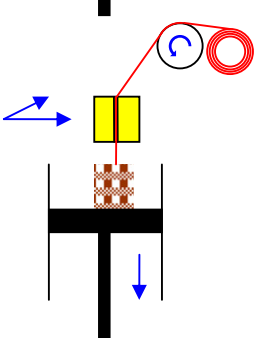
3DP was invented and patented by Michal J. Cima and co-workers (US Patent US005340656A) in 1993 and is based on conventional inkjet printing technology [9]. The single steps of 3DP are symbolically depicted in Fig. 2 in more detail. The flexibility that 3DP offers is outstanding in many aspects. From a material point of view almost any powder can be used provided it is combined with an adequate binder. Theoretically there is no limit to the combination of different powders that can be selectively solidified using various binders. The scalability of the 3DP technique enables manufacturing of large specimens in the meter range [26] as well as small specimens of a few millimeters [27]. The freedom to build up any geometry is limited only by the precision of the method and the surface quality of the parts. Importantly, the powder bed acts simultaneously as reagent and as physical support for the printed parts.

#### 3.1. Basic requirements for 3DP in scaffold engineering

Until now it has not been clear what requirements powders and binders used in 3DP should fulfill. The aim of this section is to discuss these requirements and review the present knowledge. To do so, the printing procedure is divided into single steps and explained in more detail (Fig. 3). In the first step (step 1) a counter clockwise rotating roller spreads and slightly compresses a thin and homogeneous powder layer. Then (step 2) a print head locally sprays binder droplets onto the powder bed, resulting in small craters due to the ballistic impact. The surrounding powder particles are wetted by the binder droplet (step 3). The binder drops

**Table 1**

Overview of the main SFF methods (the smallest feature refers to the smallest possible channel or pore size if not stated otherwise – for details check references).

Principle	Technique	Parameters	Features
	<b>Three-Dimensional Printing (3DP):</b> Using adhesive: The inkjet head prints droplets of a binder fluid on a powder bed. This fluid binds the powder and thus builds up part of the solid's cross section. This process is repeated for every layer until the 3D structure is printed and the remaining powder is removed.	Layer thickness: slurry method: 20–100 $\mu\text{m}$ [96] dry powder method: 50 $\mu\text{m}$ [20] Smallest feature: 350–500 $\mu\text{m}$ [47], [32]	+Broad material range +No support structure needed +Cost efficient -Small green strength -Depowdering difficult due to weak bonding between particles -Powder can be trapped inside the body
	<b>Selective Laser Sintering (SLS):</b> Using Heat: Laser beam selectively initiates melting in a thin layer of powdered material. Iterative repetition for every layer. Unmelted powder serves as support structures and remaining powder is removed.	Layer thickness: 76–100 $\mu\text{m}$ [25,97,98] Smallest feature: 45–100 $\mu\text{m}$ [25]	+High mechanical properties +No support structure needed -High processing temperature -Powder can be trapped inside the body
	<b>Stereolithography (SLA):</b> Using Light: Laser beam selectively initiates solidification in a thin layer of liquid photopolymer. Iterative repetition for every layer. Requires support structures for unconnected parts.	Layer thickness: 1 $\mu\text{m}$ for specimen volume smaller than 35 $\text{mm}^3$ [99,100] Smallest feature: Indirect: 366 $\mu\text{m}$ [101] Direct: 1–5 $\mu\text{m}$ [102] 10–70 $\mu\text{m}$ [99,103]	+High accuracy -Photopolymer needed -Support structure needed
	<b>Robocasting (RC):</b> Using Slurry: Robot controlled nozzle writes a cast or slurry directly layer by layer. Before the next layer is added the slurry must turn from a viscous paste to a solid structure by drying in order to bear the weight of the next layers.	Layer thickness: 225–750 $\mu\text{m}$ [104–106] Smallest feature: rod diameter: 200–400 $\mu\text{m}$ [107,108]	+High accuracy +No support structure needed +Combination of materials with 2 nozzles -Material limitations -Large build time -Expensive process -Geometry restricted
	<b>Fused-Deposition-Modeling (FDM)</b> Using Mold: Thermoplastic fiber is heated and selectively extruded via a nozzle layer by layer. Small feature size of scaffolds allows the fiber to bridge across unconnected parts without support structures.	Layer thickness: 250–370 $\mu\text{m}$ [109–112] Smallest feature: rod diameter: 260–700 $\mu\text{m}$ [110]	+No support structure needed +No powder trapped -Thermoplast polymers required -Mechanical anisotropy -High temperatures

continue wetting the adjacent powder particles and spread within the powder bed (step 4). Finally, (step 5) reaction between the binder and the powder particles results in local hardening and thus builds up a small piece of the final solid. These steps are iteratively repeated (step 6, analogous to step 1) until the final layer of the solid is printed. In the two last steps the green specimen is extracted from the powder bed, including the removal of excessive powder (depowdering). In the following the critical properties and requirements involved in these single steps are presented and discussed.

Flowability of the powdered material is an essential requirement for building up thin powder layers (step 1 & 6) and also to

remove the powder from the printed part (step 8). Flowability can be quantified by the flowability factor coefficient ( $ffc$ ), defined as the ratio of the consolidation stress  $\sigma_1$  and the compression strength  $\sigma_c$ , which can be reproducibly measured with a so-called Ring Shear Tester [28]. Flowability is mainly influenced by particle size and shape and can be measured quantitatively according to a standardized method [29]. High flowability allows the roller to build up thin and homogeneous layers and thus enables higher resolution in the printed solid, which is one of the scaffold requirements, as described earlier. Since resolution is generally at least twice the dimension of the powder particle size [30], a high

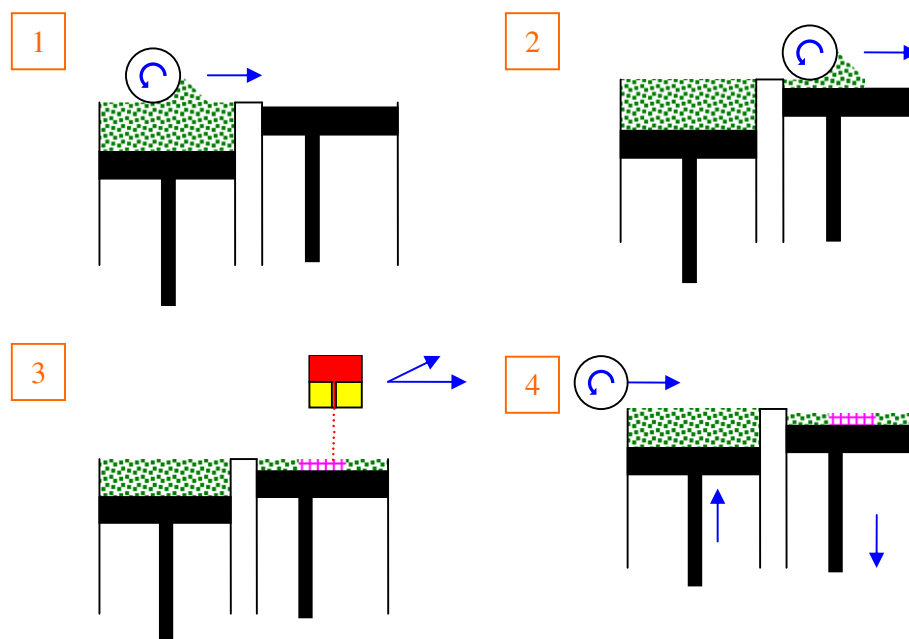


**Fig. 2.** Iterative steps in the powder-based 3DP principle. The roller places a thin layer of powder in the build area (steps 1 and 2). The inkjet head prints droplets of a binder fluid on the powder bed and thus locally solidifies part of the solid cross-section (step 3). This process is repeated for every layer until the 3D structure is printed and the remaining powder is removed (step 4).

resolution can only be achieved by using a fine powder. However, dry, fine particles tend to agglomerate, since interparticulate forces dominate gravitational forces, resulting in poor flowability [31]. Therefore, a trade-off between flowability and resolution is inevitable. Flowability is also essential for depowdering, the last step in the printing process (step 8). Low flowability hinders the removal of the powder present inside the pores and the cavities of the printed green specimen and makes depowdering a difficult and sometimes unachievable goal. Depowdering of simple cavities demands a minimum cavity diameter of five times the average powder size [32]. This value might be even higher for complex cavity systems and irregular cellular structures.

Stability of the powder is required for binder spraying and recoating. During spraying binder drops with a volume of around 30  $\mu\text{l}$  hit the loose powder bed with an approximate velocity of  $6 \text{ m s}^{-1}$  [33]. This impact leads to a crater-like depression with a binder droplet at the bottom (step 3). The powder–binder droplet interaction is illustrated in Fig. 4. Increasing the velocity increases the impact diameter at a rate of approximately 5–10  $\mu\text{m}$  per  $1 \text{ m s}^{-1}$  increase in velocity over the range used in 3DP [34]. During recoating shear forces are applied to the top layer of the powder bed. As a result, the thin printed structures may be displaced, possibly affecting the integrity and accuracy of the printed object. Besides lateral displacement, there is also a risk of vertical displacement due to compressive loads resulting from gravitational forces. For example, Lee et al. [35] measured downwards displacements of from 23 up to 260  $\mu\text{m}$  in a 76.2 mm deep powder bed. These negative effects can be reduced by increasing the cohesive strength of the powder bed, for example by adding a small amount of moisture to [36] or by increasing the packing density of the powder bed.

Wettability of the powder by the binder droplet (step 4) is another crucial requirement influencing the printing accuracy and the green strength of the printed object [37]. Specifically, too much wetting would lead to extensive binder spreading (step 5), limiting the printing resolution. In contrast, poor wetting due to a large contact angle or to a high viscosity of the binder [9] would result in poor interdigitation between neighboring printed layers and thus result in low mechanical integrity of the green body. Powder

wetting depends on many parameters, such as the contact angle between binder and powder, the binder viscosity, the topography of the powder bed surface (depending on powder shape and size) and the chemical reactions occurring between binder and powder. These reactions can lead to swelling or partial dissolution of the particles constituting the powder bed. Thus the distance over which the fluid can migrate depends not only on binder and powder properties and packing but also on the curing rate of the binder [9]. Obtaining reliable quantitative results for the contact angle of solids is challenging and greatly depends on surface characteristics [38]. For powders it is even more difficult. Many sophisticated methods, such as dynamical drop shape analysis, the capillary rise method and the floating particle method, are available to describe the interaction between binder and particles [39–41]. However, these studies also reveal that there is still a poor understanding of this field of research. So far, investigations on binder droplet impact and spreading suggest that surface tension forces are generally stronger than the cohesive strength of the powder bed, thus causing particle rearrangement and powder bed densification [42]. Capillary pressure not only draws the binder selectively into the interparticle necks but also pulls adjacent particles together to form a nearly spherical binder–particle agglomerate, hence minimizing the total surface energy of the system [36]. The timescale for absorption and dissipation have been determined to be of the order of 10–100 ms [43]. An in-depth understanding of multiple binder droplet–powder interactions and its implication on 3DP will be a matter of future research.

Reactivity of the powder with the binder [44,45] also plays a very important role in 3DP because binder spreading (step 5) would be prevented by a too high reactivity whereas a very low reactivity might favor intensive binder spreading. So, the timing and reactivity of the binder reaction are crucial to the final printing accuracy, and to the consolidation of consecutive layers [46]. For 3DP scaffolds that are to be sintered after completion there is an additional hurdle, which is that the presence of too high levels of binder might be damaging to the green body due to binder burning. Therefore, the binder concentration must be minimized [37] while still providing sufficient mechanical stability to the printed

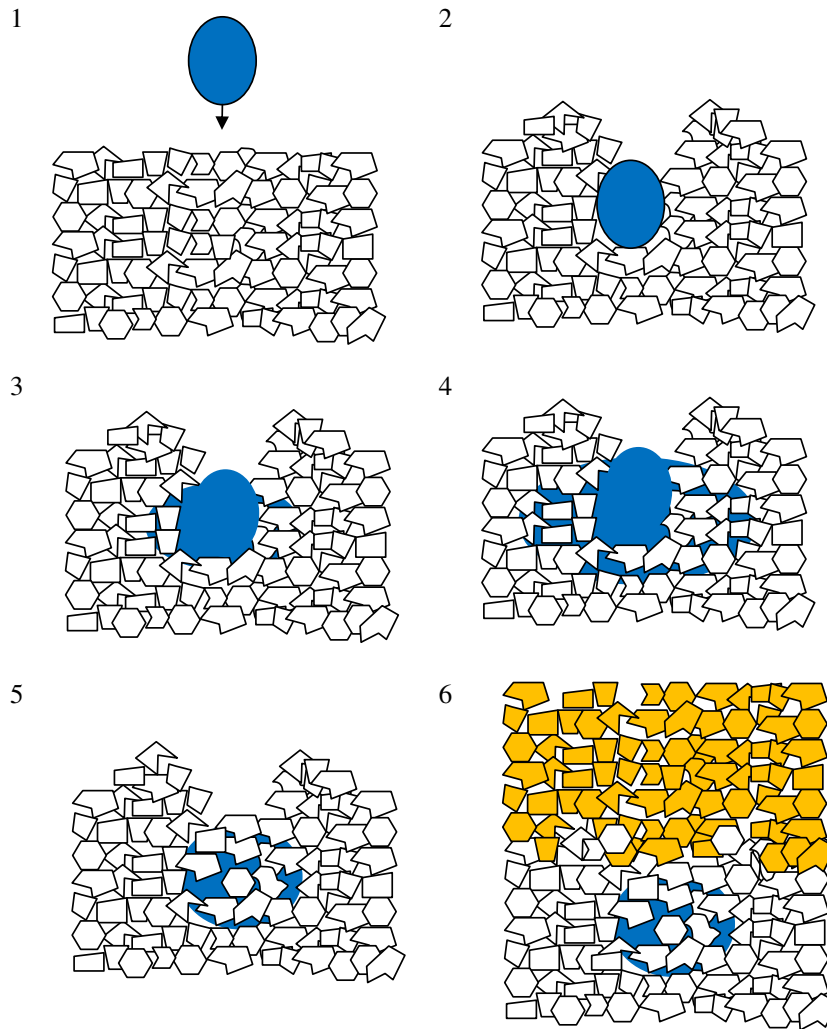


**Fig. 3.** Schematic illustration on the main stages of single binder drop powder interaction during 3DP: build-up a homogeneous thin powder layer (step 1); binder droplet delivery on the powder bed while maintaining its integrity (step 2); wetting of the powder by the binder (step 3); spreading of the drop within the powder (step 4); binder/powder reaction and hardening (step 5); recoating with a new powder layer (step 6); extraction of the green specimen from the powder bed (step 7, not depicted); removal of loose powder within the green specimen (step 8, not depicted).

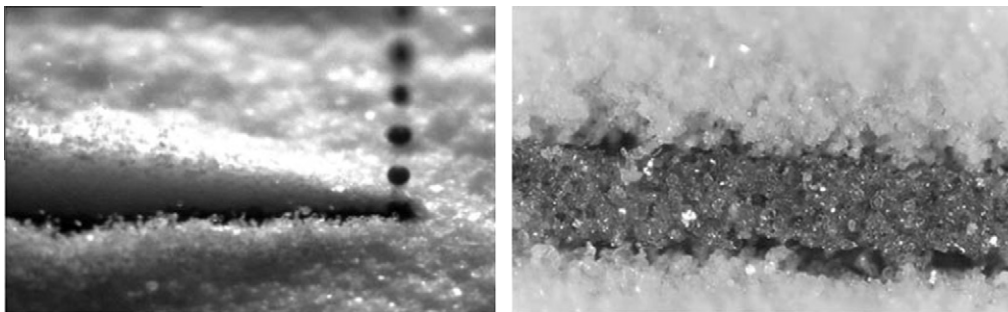


**Fig. 4.** High speed frame (left) of the droplet impact on the powder bed. Detail of a line (right) lying in the wide groove formed within the bed. (Reprinted from *Rapid Prototyping Journal*, 2003, © Emerald Group Publishing Limited, all rights reserved.)

structure. The binding mechanisms can be very different. In hydraulic cements, such as plaster of Paris or calcium phosphate cements, the powder is dissolved by the binder and the powder particles are bonded via subsequent recrystallization, as depicted in Fig. 5. In another approach hardening occurs by gluing of the powder particles using a polymer-based binder [47].

Green strength refers to the initial strength after printing and before post-processing steps, e.g. sintering. Obviously, this is a very important property of the printed scaffold and describes the mechanical characteristics immediately after extraction from the powder bed and subsequent depowdering (steps 7 and 8). Insufficient green strength may result in shape changes or ultimately in

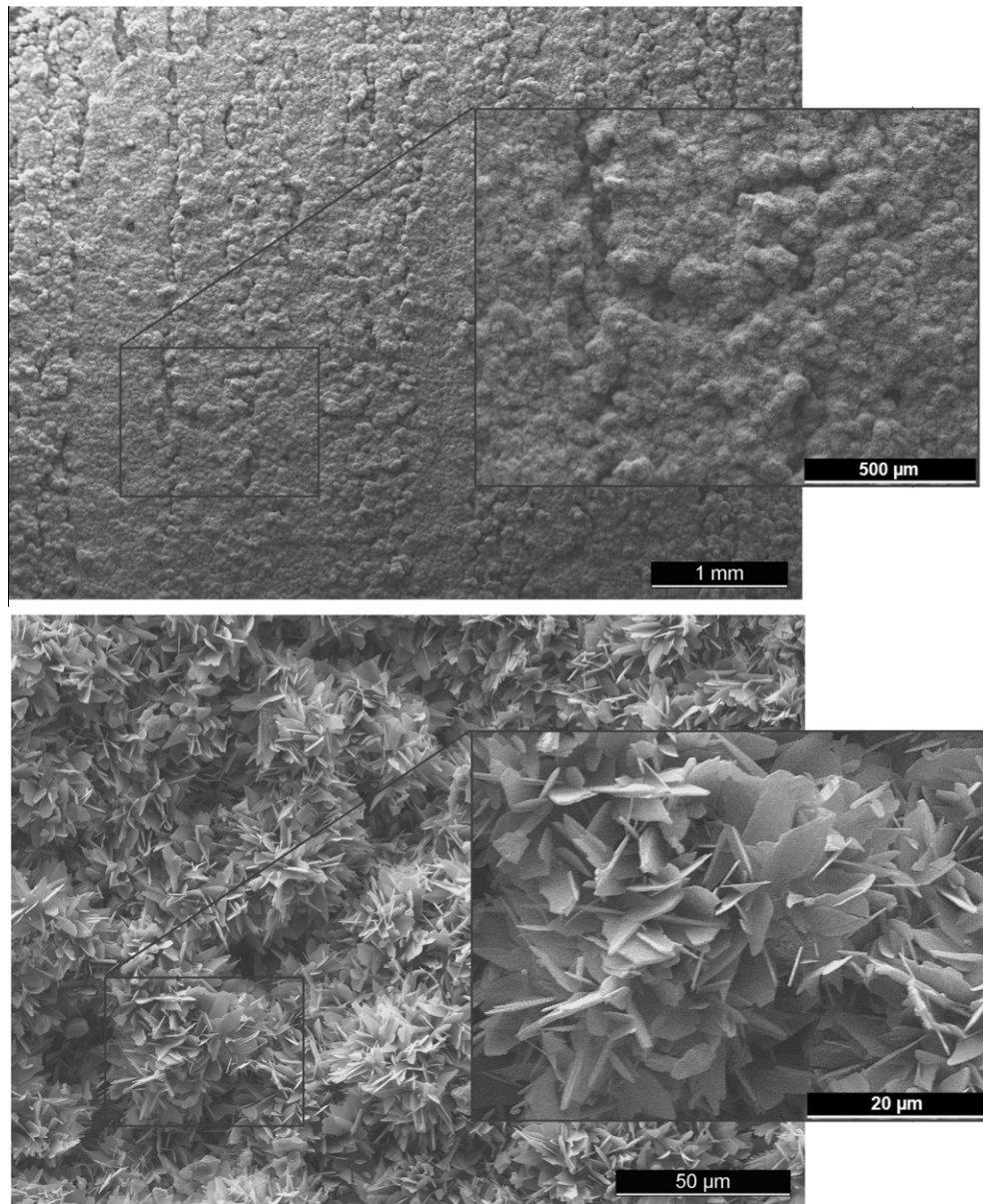


**Fig. 5.** 3DP surface structure after the reaction between TCP and the acid binder. Four enlargements of a 3D printed surface are shown.

mechanical failure of the green body. Even the weight of the unbound powder might be critical for weak scaffold structures [35]. The green strength of the printed part relies mainly on two factors: (i) the strength of the bonds between adjacent powder particles, (ii) the strength of the bonds between adjacent layers. The mechanical properties of the green body are dictated by two binding mechanisms: binder adsorption and mechanical interlocking [37]. As previously described, binder adsorption can lead to either a chemical reaction and subsequent interparticulate crystallization or be the result of an adhesive effect between the particles. Green parts finally need to be post-processed to improve their mechanical properties, for example by dipping them in binder solution [48] or by sintering [49]. In both cases the shape of the printed solid may change. Optimal green strength is required to meet the mechanical property demands of scaffolds, since the green strength will affect the final strength [50]. In general, a higher apparent density results in better mechanical properties [51]. Rapid vascularisation of scaffolds is, however favored, by more porous, and therefore weaker, structures [20]. With a random

arrangement of large single sized spherical particles an apparent density of no more than 64% can be achieved [52]. This results in high porosity and low mechanical integrity of the printed green parts. Bimodal powder mixtures are used to tailor the apparent density and to optimize the conflicting requirements of high porosity and mechanical integrity [20].

### 3.2. Materials used in powder-based 3DP for bone scaffold tissue engineering

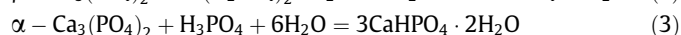
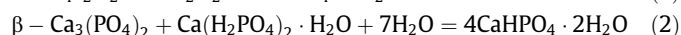
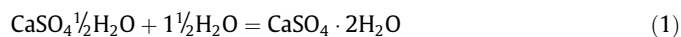
A crucial advantage of 3DP is the wide range of materials that can be used, from synthetic and natural polymers to ceramics, as well as composites of the aforementioned [53]. The sole condition is availability of the material in powder form. Table 2 summarizes the different material approaches (polymeric, ceramic and composites) used in the field of bone scaffold engineering. This table is ordered by particle size, due to the importance of particle size for high resolution 3DP.

**Table 2**  
Materials in powder-based 3DP ordered by particle size according to literature. *Abbreviations:* I: Impregnation; d50: mean particle size;  $\alpha/\beta$ -TCP: alpha/beta-Tricalcium Phosphate; TTCP: Tetracalcium phosphate; CPP: Calcium Polyphosphate; HA: Hydroxy-Apatite; PE: Polyethylene; PCL: Polycaprolactone; PLLA: Poly-L-Lactic Acid; PVA: Polyvinyl alcohol.

Powder		Binder	References
Material	Particle size [ $\mu\text{m}$ ]		
<i>Polymers</i>			
Natural polymers	20–150	100% water	[54,55]
PCL/PE oxide	45–150	5% and 20% chloroform	[113]
PLLA	75–150	100% chloroform	[56,114]
UHMWPE/Maltodextrin	100–150	100% water	[115]
<i>Ceramic</i>			
$\beta$ -TCP	16 (d50)	25% oxalic and tartaric acid	[116]
TCP/TTCP	10–20	10–20% phosphoric acid	[62]
$\beta$ -TCP	30	5–10% phosphoric acid	[48]
TTCP/ $\beta$ -TCP	<100	25% citric acid	[46]
$\alpha$ -TCP	10 (d50)	5% sodium chondroitin sulphate 12% disodium succinate 83% distilled water	[63]
<i>Composite</i>			
TCP/TTCP/Polymer (I)	10–20	10–20% phosphoric acid Polymer solutions of dichloromethane 10–50 wt.% (I)	[71]
$\beta$ -TCP/Bioglass	7 & 41 (d50)	Orthophosphoric & pyrophosphoric acid	[117]
HA/Starch	4 & 50 (d50)	94.5% distilled water 2.5% glycerin 3% rest	[20]
HA	69 (d50)	14% schelofix64 5% polyvinyl alcohol	[29]
CPP/PVA	75–150	Zb 58 10 wt.% PVA	[84]
HA/Maltrodextrin	38–83	Water-based	[50]
HA & Maltrodextrin /apatite-wollastonite glass	3–5 & 90–100/ 88 (d50)	Water-based	[69]

Polymeric materials can be subdivided into synthetic polymers and natural polymers. Natural polymers, such as polysaccharides, are generally extracted from plants (starch, dextrose, cellulose, etc.) and animals (sodium hyaluronate, collagen, etc.), even though most polymers can now be synthesized chemically or biotechnologically (e.g. microbial production of sodium hyaluronate). These polymers are generally hydrophilic and can be used in combination with water-based and solvent-free binders. Thus, various blends of powdered natural polymers are adequate for printing scaffolds used in medical applications [54,55]. Synthetic polymers, on the other hand, can be customized to the actual need. However, synthetic polymers are often poorly soluble in aqueous media, meaning that organic solvents, e.g. chloroform, must be used, raising biocompatibility issues. These toxic solvents evaporate rather fast, while dissolving some of the polymer particles. Great effort has been invested into this approach [6,56]. After 1 week of drying 0.5 wt.% (5000 p.p.m.) chloroform remained on samples made by 3DP. Chloroform extraction techniques reduced the level of chloroform below 50 p.p.m. [57], however, there is always the risk of finding toxic solvent residues in the printed scaffold [58]. Furthermore, the use of solvents represents a burden when considering large-scale commercial production of medical grade biomaterials. With ceramic powders two main approaches can be considered. In the first approach the ceramic powders remain passive and the green body strength results from the binder properties [29,59]. Since this approach implies the use of polymeric binders, such scaffolds are classified as composite materials and will be discussed in more detail in the composite section. In the second approach hydraulic cements are used [60,61]. In other words, the binder dissolves the powder particles and new crystals form and interdigitate to form a stiff ceramic network. One of the most intensively studied materials is calcium sulfate hemihydrate, also called plaster of Paris. Upon reaction gypsum is formed (Eq. (1)). Several calcium phosphate cement formulations have also been considered [62,63]. Since these formulations must react rapidly,

highly reactive compounds such as  $\alpha$ -tricalcium phosphate ( $\alpha$ -TCP,  $\alpha$ - $\text{Ca}_3(\text{PO}_4)_2$ ), tetracalcium phosphate (TetCP,  $\text{Ca}_4(\text{PO}_4)_2\text{O}$ ), monocalcium phosphate monohydrate (MCPM,  $\text{Ca}(\text{H}_2\text{PO}_4)_2 \cdot \text{H}_2\text{O}$ ) are used with phosphoric acid as the binder. Here some examples of setting reactions are provided:



Eqs. (2) and (3) are often referred as the brushite cement reaction [64]. Brushite is also referred to as dicalcium hydrogen phosphate dihydrate (DCPD,  $4\text{CaHPO}_4 \cdot 2\text{H}_2\text{O}$ ). Acid binders such as phosphoric acid and citric acid are usually used in 3DP with ceramic powders. These binders initiate a setting reaction as described above. Small amounts of unreacted binder residuals are generally not critical. Some of them (citric acid, phosphoric acid and oxalic acid) are present in our body and can be easily removed [65]. Tartaric acid is metabolically inert in the human body. The use of these acids with calcium phosphates is widespread in the literature [66,67]. The fragile green stability based on this cement reaction can be improved by either a post-print hardening regime (e.g. immersing samples in phosphoric acid) or by sintering, leading to thermal decomposition of the brushite phase and formation of a pyrophosphate [48]. The use of  $\alpha$ -TCP, TetCP and DCPD mixtures has also been suggested for the fabrication of printed apatite scaffolds [61,68]. Composite materials used for 3DP can be found in the literature using various combinations of ceramic, bioglass or polymeric components. Two main approaches can be distinguished: composites that are formed during and those that are formed after the printing process. A solution of a soluble polymeric binder [29,59] is used to locally wet ceramic particles and glue them together through drying. After the printing process the part is depowdered and the organic binder removed during sintering by pyrolysis [59]. Another option is the use of an initial blend of a ceramic and

a polymer powder. The binder sprayed onto the particles dissolves the polymer and hardening is caused by precipitation of the polymer during binder drying [20,50,69]. The mechanical properties of the green body can be improved by adding an additional phase. One example is apatite-wollastonite (A-W) bioglass, which contains crystalline oxyfluoroapatite ( $\text{Ca}_{10}(\text{PO}_4)_6(\text{O},\text{F}_2)$ ) and  $\beta$ -wollastonite ( $\text{CaO}\cdot\text{SiO}_2$ ) in a  $\text{MgO}\text{-CaO}\text{-SiO}_2$  glassy matrix [70]. 3D printed ceramic A-W bioglass composites have promising mechanical properties and were shown to be non-toxic and more prone to form hydroxyapatite at their surface when soaked in simulated body fluid [69]. Second, composites can be formed after the printing process. This approach relies on the infiltration or impregnation of a monomer solution (e.g. dianhydro-D-glucitol [bis(dilactoylmethacrylate)] DLM-1 [46]) into the printed solid. Hardening is achieved by curing the monomer into a polymer. A polymer solution can also be used. For example, Gbureck et al. impregnated their printed solids with a dichloromethane-PLA/PGA polymer solution [71]). An interesting aspect of this approach is that the polymer matrix can be drug loaded and the release kinetics can be tailored with the degradation rate of the polymer [71]. It remains, however, a challenge to fully impregnate the samples and at the same time maintain a suitable porous network. Additionally, impregnation using toxic solvents raises the issues mentioned in Section 3.2. For the first approach the polymeric binders are removed by pyrolysis during sintering. However, remaining residuals from this process can also be critical to the biocompatibility of the final scaffold.

### 3.3. Structural and mechanical properties of 3D printed ceramic scaffolds

Calcium phosphate-based ceramics have a long history and are widely used in synthetic bone replacement due to their chemical similarity to bone mineral [72,73]. Calcium orthophosphates have been studied as bone repair materials for more than 80 years [60]. In contrast to metals and polymers, several calcium phosphates spontaneously bind to living bone [74] and therefore their use as 3DP of bone scaffolds is self-evident. Calcium phosphates differ in their Ca/P molar ratio (hydroxyapatite (HA), 1.67;  $\alpha/\beta$ -TCP, 1.5) and basicity (TetCP is basic, MCPM is acidic), resulting in different solubilities and resorption rates [60]. Due to the importance of calcium phosphates in bone scaffold engineering the structural

and mechanical parameters governing 3DP of calcium phosphate scaffolds are summarized in Table 3.

As previously discussed, the ideal scaffold mimics not only the structure but also the load-bearing capacity of the extracellular matrix of bone. Therefore, the mechanical properties of calcium phosphates are of major importance and are discussed in detail as compared with bone.

The mechanical properties of calcium phosphates greatly depend on their porosity and structure. Dense HA has compressive and flexural/tensile strengths reported to be in the ranges 430–920 and 17–110 MPa, respectively [75]. For comparison, cortical and cancellous bone present lower values in the ranges 100–230 and 2–12 MPa for compressive strength and 50–150 and 10–20 MPa for flexural/tensile strength, respectively [75]. However, HA is much less resilient than bone: the fracture toughness of HA is close to  $1 \text{ MPa m}^{1/2}$ , compared with 2–12  $\text{MPa m}^{1/2}$  for cortical bone [15,75]. Due to the brittleness of calcium phosphates their use is limited to non-load-bearing applications [76].

The mechanical properties required for powder-based 3DP of ceramic scaffolds are even more critical, since typically the initial green strength of the printed part is provided by interdigitation of calcium phosphate crystals only. While the intercrystalline space provides a highly specific surface and excellent osteoconductivity [60], the weak bonding within the green body might result in damage to the filigree design features during depowdering. However, post-print hardening or aqueous conversion may be used to increase the compressive strength 3- to 4-fold, resulting in strengths higher than the values reported for commercial sintered bone graft substitutes [62]. Depending on the post-print treatment of the 3DP structure, compression strength may vary significantly between 1 and 77 MPa (Table 3). A trade-off between mechanical and structural parameters is inevitable.

At the same time, the structural properties are vital factors in scaffold-cell interactions. The turning point of scaffold seeding in vivo is the transition from an inert structural backbone to a vascularized construct [20]. Classical scaffold designs take this concept into account with highly open porous designs relying on neovascularization of the scaffold from the surrounding tissues. However, this approach is critical, due to a limited cell penetration depth. It remains a challenge to seed scaffolds with cells and maintain cell viability for prolonged periods. Mineralization of seeded

**Table 3**

Comparison of the structural and mechanical parameters governing 3DP of calcium phosphate scaffolds. The list is ordered by the achievable layer thickness of the 3DP process. Resolution is either defined by the diameter of the macropores (MP), the indicated manufacturing tolerance (MT) or the smallest feature size (FS).

Architecture Design/MP	Structural			Mechanical			References
	Layer thickness [ $\mu\text{m}$ ]	Resolution [ $\mu\text{m}$ ]	Porosity/Pore size [%/ $\mu\text{m}$ ]	Compressive green strength [MPa]	Compressive sintered strength [MPa]	Posttreatment	
Custom	50	1000 (MP)	30–64% 0.3–0.4 $\mu\text{m}$ 10–20 $\mu\text{m}$	–	31	–	[20]
CT based /Cylindrical	88	$\pm 50$ (MT) 750 (MP)	35–40%	–	3–4	–	[85,116]
Custom	89	–	77–79%	0.1–0.2	0.2–0.4	–	[118,119]
Cylindrical P	100	$\pm 200$ (MT)	27–39% (green) 3–7% (sintered)	2.8	0.8–4 25–45 (hardening via immersion)	$3 \times 30 \text{ s}$ in 20% $\text{H}_3\text{PO}_4$ (hardening)	[48]
CT based /Cylindrical P	100	$\pm 100$ (MT)	61% 10 $\mu\text{m}$	18.6	–	–	[63]
Cylindrical P	100	500 (MP)	36–50%	0.6–0.7 76.1 (Infiltrated)	4.3	DLM-1 (Infiltration Polymer)	[46]
Custom	100	–	52% ( $T_{\text{sint}}: 1.2 \text{ k}^\circ\text{C}$ ) 3–30% ( $T_{\text{sint}}: 1.3 \text{ k}^\circ\text{C}$ )	1.3 (Flexural strength)	77 (Flexural strength)	–	[69]
Solid Cylinder	150	$\pm 100$ (MT)	35% 53 $\mu\text{m}$	–	34	–	[84]
Solid Block	175	–	59–65 $\mu\text{m}$	ca.0.2–0.7	ca.1.45	–	[50]
Quadratic channels	200–300	330–450 (FS)	10–30 $\mu\text{m}$	–	22	–	[59]

osteoblasts have been reported up to a depth of 100–300  $\mu\text{m}$  into a scaffold [77]. Cell seeding on the scaffold periphery might not only act as a barrier to nutrient diffusion but also hinder further cell migration [57].

Several *in vitro* investigations of 3D printed parts with human cells (osteoblasts, periosteal cells) have shown good biocompatibility of calcium phosphate-based scaffolds [10,78]. A recent study analyzed whether and how 3D printed calcium phosphate surfaces can be resorbed by osteoclast-like cells [79]. Measured cell proliferation and cell viability indicated good *in vitro* biocompatibility. Osteoclast-like cells were able to resorb calcium phosphate surfaces, even showing large resorption lacunae on biphasic HA/TCP specimens. In numerous animal (rats and goats) studies various 3D printed ceramic scaffolds were implanted intramuscularly as well as on and in bone, showing good biocompatibility and osteoinductivity *in vivo* [20,78,80,81]. Comparisons with xenografts and autografts have shown promising results for 3D printed scaffolds.

The interior of 3DP scaffolds requires pores on two different scales. According to Karageorgiou [22] macroporosity (pore size  $>50 \mu\text{m}$ ) has a strong impact on osteogenic outcomes. Conversely, microporosity (pore size  $<10 \mu\text{m}$ ) is also a key factor, leading to a higher specific surface area and thus higher bone-inducing protein adsorption, as well as to ion exchange and bone-like apatite formation by dissolution and reprecipitation [22].

The exterior of the scaffold is limited by the layer thickness of the 3DP process (determining 3DP resolution in the vertical direction) and by the powder grain size (determining the surface roughness of the final part). The scaffold architecture can vary from simple cylinders to complex irregular shaped bone grafts, depending on the application. Fig. 6 depicts a 3D printed calcium phosphate structure. The layer thickness for this example was 89  $\mu\text{m}$  and can be clearly identified as a limiting factor for high resolution.

Post-processing can also have a major effect on the structural properties of the printed scaffolds. While certain post-processing

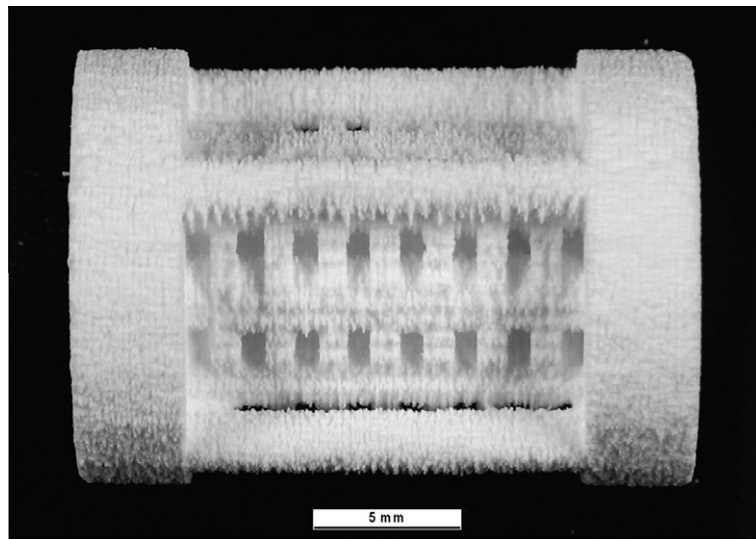


Fig. 6. 3D printed calcium phosphate scaffold.

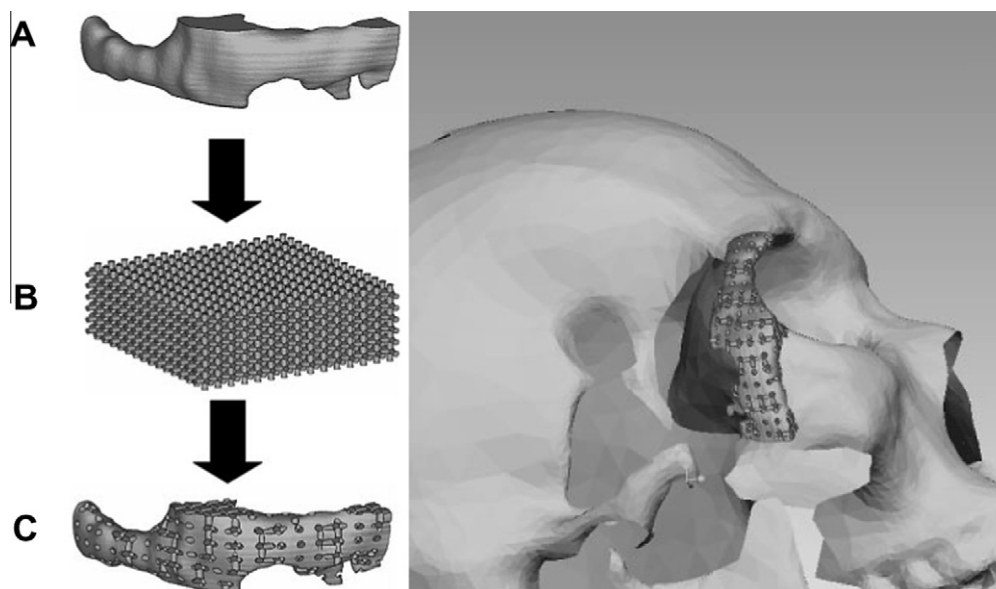


Fig. 7. Virtual construction steps of 3D printed skull scaffold. (Reprinted from *Materialwissenschaft und Werkstofftechnik*, © 2006, permission from Wiley being sought.)

steps, such as infiltration or post-print hardening, will not have a critical impact on the structural properties, sintering certainly will. Sintering is a complex process dependent on many factors, such as time, temperature, particle size and material properties of the powders. Sintering has an impact on the composition (e.g. phase changes), mechanical properties (e.g. hardening) and structural properties (e.g. shrinkage) of the materials. Due to large voids between the particles in the green state, significant sintering shrinkage by up to 32% [82,83] can occur. Since shrinkage is highly reproducible it can be compensated for by scaling the initial CAD model prior to printing. Dimensional changes in the green and sintered stages are used to determine the correction factor. Registering CT images with their 3D printing matrices yields almost isotropic shrinkage [83]. Applying these corrections, dimensional accuracy in the region of 100  $\mu\text{m}$  is feasible, in spite of sintering shrinkage [84].

The geometrical freedom inherent in 3DP also allows sophisticated macro design of scaffolds to fit complex bony defects based on CT scans. A common approach is the volumetric subtraction of CT based solids (Fig. 7) with a cylindrical lattice structure resulting in a porous structure with the appropriate initially determined outer dimensions [63,85]. Details of this sophisticated method are well described in literature [8,86,87] and can be summarized as follows. The first step consists of non-invasive imaging data acquisition, typically via CT or magnetic resonance imaging. Different tissues in this dataset are then differentiated through contrast segmentation, followed by reconstruction of the segmented slices into a 3D model. An accurate voxel-based 3D model can represent the scanned anatomy, however, it cannot be effectively used for further modeling, since the direct conversion of medical imaging data into a solid CAD model is not a simple task [8]. In the CAD model the defect can be filled and exported in a special .stl data format in common use in SFF.

#### 4. Outlook

3DP is a highly versatile method allowing nearly unlimited designs and a large variety of materials to be used for scaffold engineering. Apart from these promising possibilities, major challenges and limiting factors are addressed and potential strategies to improve 3DP for scaffold engineering are proposed in the following. Recalling the long-term goal of scaffold engineering as temporarily mimicking the structural and mechanical properties of the natural extracellular matrix of bone as closely as possible, the following challenges and limitations have been uncovered. From an engineering point of view, the low resolution of the 3DP method and the inadequate mechanical properties materials produced by 3DP need to be mentioned. From a biological perspective, the conventional tissue engineering approach of seeding the scaffold with

cells raises critical issues concerning the long-term viability of the cells inside the scaffolds.

On the biological level, novel approaches, termed intrinsic vascularisation, use vascular induction from the core of the scaffold to the periphery due to bioactive matrix and vessel driven angiogenesis [20,88]. This goal can be achieved using inorganic (copper II) and organic angiogenic factors (e.g. vascular endothelial growth factor VEGF) specifically deposited at the end of a closed pore [62,89]. Both approaches show great potential for neovascularization in animal models and will enhance future research in 3DP of scaffolds.

On the engineering level, the composite approach seems to be promising for the generation of less brittle ceramic bone scaffolds capable of bearing a load and inducing physiological strain in cells. Scientific achievements in the field of bioinspired materials [18] have given rise to new approaches to the formation of more ductile ceramic-based composite bone scaffolds. Highly organized structures in nature (e.g. teeth and the nacreous layer of mollusk shells) have mechanical properties that until today have been unachievable by scaffold engineering. A step into this direction lies in realizing functionally graded materials with local variations in the material composition [90,91]. Another key factor needed to achieve this goal is high spatial resolution, allowing a high level of detail. This implies fine powder particles (a thin layer thickness) with high flowability (enabling the recoating step). This is a non-trivial aspect, especially for polymeric particles. Due to their ductile behavior, milling with a reasonable yield of polymer is hard to achieve. Although powdered ceramics with the desired particles sizes are available, there is a lack of systematic knowledge about the optimal size and geometry of particles for 3DP.

Plasma treatment of the powder particles [92] can enhance the flowability of fine particles, opening up a new path to thin powder layers and thus the high level resolution currently not achieved by traditional 3DP. Fig. 8 illustrates the high flowability of a 5  $\mu\text{m}$   $\beta$ -TCP powder.

Apart from powder characteristics, high resolution is mainly determined by the binder droplet size. Whereas in the past SFF was limited to high end research applications, today SFF and printing technology is experiencing a massive expansion. This has led to significant technological innovations, e.g. in the development of fast and reliable print heads. Today, commercially available print heads are able to spray binder droplets of a few picoliters. This innovation explosion will open up new research opportunities in the field of 3DP for scaffold engineering.

Critical engineering assessment of 3DP accuracy and precision with sophisticated, quantitative imaging techniques and an adequate statistical assessment of precision and reproducibility are essential for further improvement. High resolution CT [17,93] scans will allow local quantitative analysis of scaffolds and, with



Fig. 8. High flowability of plasma treated 5  $\mu\text{m}$  powder (left) and a homogeneous bed of the same powder (right).

that, monitoring of the mineralization process. For a further understanding of micro- and macro mechanical properties, image-guided failure assessment [94,95] will give further insights in the mechanical behavior of these materials under stress.

## 5. Conclusion

In this paper the current state of knowledge in the field of powder-based 3DP for bone scaffold engineering has been reviewed. The advantages 3DP include a wide variety of materials, provided in powdered form, and geometrical freedom, restricted only by the resolution of the method. The process is easily scalable and reasonably rapid, making it valuable for systematic research and industrial scaffold applications. In particular, the field of powdered materials and binders used for 3DP was reviewed and discussed. Furthermore, a comprehensive review of powder-based 3DP of ceramics has been undertaken. Finally, the outlook for and possible developments in the rapidly growing field of SFF for tissue engineering was described.

The principle of successive layer by layer manufacturing is in line with the engineering approach of dividing a complex issue into simple manageable pieces. In this spirit, the solid part of one layer is likewise broken into smaller pieces, the powder particles. Only if the single powder particles are bound together can a new solid be created. In this sense only an interdisciplinary approach between “tissue-related fields” like biology and biochemistry and the “engineering-related fields” of biomaterials and biomechanics will bring further insights and progress in “tissue engineering”. Even though such an interactive collaboration will inspire major steps in the field of tissue engineering, the comparison with nature’s underlying perfection will hopefully result in a humble attitude. In the words of Isaac Newton:

“I do not know what I may appear to the world; but to myself I seem to have been only like a boy playing on the sea-shore, and diverting myself in now and then finding a smoother pebble or a prettier shell than ordinary, whilst the great ocean of truth lay all undiscovered before me”.

## Acknowledgment

Funding from the RMS Foundation is gratefully acknowledged.

## Appendix A. Figures with essential colour discrimination

Certain figures in this article, particularly Figures 1,2,3,8 are difficult to interpret in black and white. The full colour images can be found in the on-line version, at doi: 10.1016/j.actbio.2010.09.039

## References

- [1] Langer R, Vacanti JP. Tissue engineering. *Science* 1993;260(5110):920–6.
- [2] Griffith LG, Naughton G. Tissue engineering – current challenges and expanding opportunities. *Science* 2002;295(5557):1009.
- [3] Koerner C. In: Körner C, editor. *Integral Foam Molding of Light Metals: Technology, Foam Physics and Foam Simulation*. Berlin: Springer Verlag; 2008.
- [4] Hollister SJ. Porous scaffold design for tissue engineering. *Nat Mater* 2005;4(7):518–24.
- [5] Mathieu LM, Mueller TL, Bourban PE, Pioletti DP, Muller R, Manson JAE. Architecture and properties of anisotropic polymer composite scaffolds for bone tissue engineering. *Biomaterials* 2006;27(6):905–16.
- [6] Zeltinger J, Sherwood JK, Graham DA, Mueller R, Griffith LG. Effect of pore size and void fraction on cellular adhesion, proliferation, and matrix deposition. *Tissue Eng* 2001;7(5):557–72.
- [7] Bohner M, van Lenthe GH, Grunfelder S, Hirsiger W, Evison R, Muller R. Synthesis and characterization of porous beta-tricalcium phosphate blocks. *Biomaterials* 2005;26(31):6099–105.
- [8] Sun W, Starly B, Nam J, Darling A. Bio-CAD modeling and its applications in computer-aided tissue engineering. *Comput -Aided Des* 2005;37(11):1097–114.
- [9] Sachs E, Cima M, Williams P, Brancazio D, Cornie J. 3-dimensional printing–rapid tooling and prototypes directly from a CAD model. *J Eng Ind Trans ASME* 1992;114(4):481–8.
- [10] Warnke PH, Seitz H, Warnke F, Becker ST, Sivananthan S, Sherry E, et al. Ceramic scaffolds produced by computer-assisted 3D printing and sintering: characterization and biocompatibility investigations. *J Biomed Mater Res* 2010;93B(1):212–7.
- [11] Dornblüth O. *Pschyrembel Klinisches Wörterbuch*. Berlin: De Gruyter; 2004.
- [12] Gibson LJ. Biomechanics of cellular solids. *J Biomech* 2005;38(3):377–99.
- [13] Wolff J. *Das Gesetz der Transformation der Knochen*. Berlin: Hirschwald; 1892.
- [14] Wegst UGK, Ashby MF. The mechanical efficiency of natural materials. *Philosophical Magazine* 2004;84(21):2167–81.
- [15] Huttmacher DW, Schantz JT, Lam CFX, Tan KC, Lim TC. State of the art and future directions of scaffold-based bone engineering from a biomaterials perspective. *J Tissue Eng Regen Med* 2007;1(4):245–60.
- [16] Rho JY, Kuhn-Spearing L, Zioupos P. Mechanical properties and the hierarchical structure of bone. *Med Eng Phys* 1998;20(2):92–102.
- [17] Schneider P, Voide R, Stampanoni M, Muller R. Post-processing technique for improved assessment of hard tissues in the submicrometer domain using local synchrotron radiation-based computed tomography. *Biomed Technol* 2009;54(1):48–54.
- [18] Bonderer LJ, Studart AR, Gauckler LJ. Bioinspired design and assembly of platelet reinforced polymer films. *Science* 2008;319(5866):1069–73.
- [19] Huttmacher DW. Scaffolds in tissue engineering bone and cartilage. *Biomaterials* 2000;21(24):2529–43.
- [20] Will J, Melcher R, Treul C, Travitzky N, Kneser U, Polykandriotis E, et al. Porous ceramic bone scaffolds for vascularized bone tissue regeneration. *J Mater Sci Mater Med* 2008;19(8):2781–90.
- [21] Bohner M, Baumgart F. Theoretical model to determine the effects of geometrical factors on the resorption of calcium phosphate bone substitutes. *Biomaterials* 2004;25(17):3569–82.
- [22] Karageorgiou V, Kaplan D. Porosity of 3D biomaterial scaffolds and osteogenesis. *Biomaterials* 2005;26(27):5474–91.
- [23] Lu JX, Flautre B, Anselme K, Hardouin P, Gallur A, Descamps M, et al. Role of interconnections in porous bioceramics on bone recolonization in vitro and in vivo. *J Mater Sci Mater Med* 1999;10(2):111–20.
- [24] Bignon A, Chouteau J, Chevalier J, Fantozzi G, Carret JP, Chavassieux P, et al. Effect of micro- and macroporosity of bone substitutes on their mechanical properties and cellular response. *J Mater Sci Mater Med* 2003;14(12):1089–97.
- [25] Leong KF, Cheah CM, Chua CK. Solid freeform fabrication of three-dimensional scaffolds for engineering replacement tissues and organs. *Biomaterials* 2003;24(13):2363–78.
- [26] Monolite UK Ltd. d-Shape, the mega scale free-form printer of buildings. <http://www.d-shape.com/>.
- [27] Lu K, Reynolds WT. 3DP process for fine mesh structure printing. *Powder Technol* 2008;187(1):11–8.
- [28] Schulze D. Flowability of bulk solids—definition and measuring principles. *Chem Eng Technol* 1995;67(1):60–8.
- [29] Irsen SH, Leukers B, Hockling C, Tille C, Seitz H. Bioceramic granulates for use in 3D printing: process engineering aspects. *Materialwiss Werkstofftech* 2006;37(6):533–7.
- [30] Vacanti JP, Cima LG, Cima MJ. 2001. Vascularized tissue regeneration matrices formed by solid free form fabrication techniques US Patent 6176874.
- [31] Zimmermann I, Eber M, Meyer K. Nanomaterials as flow regulators in dry powders. *Z Phys Chem Int J Res Phys Chem Chem Phys* 2004;218(1):51–102.
- [32] Curodeau A, Sachs E, Caldarise S. Design and fabrication of cast orthopedic implants with freeform surface textures from 3-D printed ceramic shell. *J Biomed Mater Res* 2000;53(5):525–35.
- [33] Creagh LT, McDonald M. Design and performance of inkjet print heads for non-graphic-arts applications. *MRS Bull* 2003;28(11):807–11.
- [34] Arthur TL. *Factors Limiting the Surface Finish of Three Dimensional Printed Parts*. Cambridge, MA: Massachusetts Institute of Technology; 1996.
- [35] Lee SJJ, Sachs E, Cima M. Layer position accuracy in powder-based rapid prototyping. *Rapid Prototyping J* 1995;1(4):24–37.
- [36] Sachs EEA. Three dimensional printing: The physics and implications of additive manufacturing. *CIRP Annals* 1993;42:257–60.
- [37] Uhland SA, Holman RK, Morissette S, Cima MJ, Sachs EM. Strength of green ceramics with low binder content. *J Am Ceram Soc* 2001;84(12):2809–18.
- [38] Spori DM, Drobek T, Zurcher S, Ochsner M, Sprecher C, Muehlebach A, et al. Beyond the lotus effect: roughness, influences on wetting over a wide surface-energy range. *Langmuir* 2008;24(10):5411–7.
- [39] Lazghab M, Saleh K, Pezron I, Guigon P, Komunjer L. 2004. Wettability assessment of finely divided solids. In: *Proceedings of the 4th French Meeting on Powder Science and Technology*. pp. 79–91.
- [40] Chau TT. A review of techniques for measurement of contact angles and their applicability on mineral surfaces. *Miner Eng* 2009;22(3):213–9.
- [41] Hogeckamp S, Pohl M. Methods for characterizing wetting and dispersing of powder. *Chem Ing Tech* 2004;76(4):385–90.
- [42] Lauder A, Cima MJ, Sachs E, Fan T. 3-Dimensional printing–surface finish and microstructure of rapid prototyped components. In: Rhine WE, Shaw TM, Gottschall RJ, Chen Y, editors. *Symposium on Synthesis and Processing of Ceramics Scientific Issues*, at the 1991 Meeting of the Materials Research Society. Boston, MA: Materials Research Society; 1991. p. 331–6.

- [43] Wu BM, Cima MJ. Effects of solvent–particle interaction kinetics on microstructure formation during three-dimensional printing. *Poly Eng Sci* 1999;39(2):249–60.
- [44] Bohner M. Reactivity of calcium phosphate cements. *J Mater Chem* 2007;17(38):3980–6.
- [45] Bohner M, Brunner TJ, Stark WJ. Controlling the reactivity of calcium phosphate cements. *J Mater Chem* 2008;18(46):5669–75.
- [46] Khalyfa A, Vogt S, Weisser J, Grimm G, Rechtenbach A, Meyer W, et al. Development of a new calcium phosphate powder-binder system for the 3D printing of patient specific implants. *J Mater Sci Mater Med* 2007;18(5):909–16.
- [47] Leukers B, Gulkan H, Irsen SH, Milz S, Tille C, Schieker M, et al. Hydroxyapatite scaffolds for bone tissue engineering made by 3D printing. *J Mater Sci Mater Med* 2005;16(12):1121–4.
- [48] Gbureck U, Hoelzel T, Biermann I, Barralet JE, Grover LM. Preparation of tricalcium phosphate/calcium pyrophosphate structures via rapid prototyping. *J Mater Sci Mater Med* 2008;19(4):1559–63.
- [49] Irsen SH, Leukers B, Bruckschen B, Tille C, Seitz H, Beckmann F, et al. Image-based analysis of the internal microstructure of bone replacement scaffolds fabricated by 3D printing. *Progress in Biomedical Optics and Imaging - Proceedings of SPIE*. 2006; 6318.
- [50] Chumnanklang R, Panyathanmaporn T, Sittthiseripratip K, Suwanprateeb J. 3D printing of hydroxyapatite: effect of binder concentration in pre-coated particle on part strength. *Mater Sci Eng C Biomimetic Supramol Syst* 2007;27(4):914–21.
- [51] Gbureck U, Hozel T, Klammert U, Wurzler K, Muller FA, Barralet JE. Resorbable dicalcium phosphate bone substitutes prepared by 3D powder printing. *Adv Funct Mater* 2007;17(18):3940–5.
- [52] German RM, Bulger M. A model for densification by sintering of bimodal particle-size distributions. *Int J Powder Metall* 1992;28(3):301–11.
- [53] Yeong WY, Chua CK, Leong KF, Chandrasekaran M. Rapid prototyping in tissue engineering: challenges and potential. *Trends Biotechnol*. 2004;22(12):643–52.
- [54] Lam CXF, Mo XM, Teoh SH, Hutmacher DW. Scaffold development using 3D printing with a starch-based polymer. *Mater Sci Eng C-Biomimetic Supramol Syst* 2002;20(1–2):49–56.
- [55] Suwanprateeb J. Improvement in mechanical properties of three-dimensional printing parts made from natural polymers reinforced by acrylate resin for biomedical applications: a double infiltration approach. *Polym Int* 2006;55(1):57–62.
- [56] Giordano RA, Wu BM, Borland SW, Cima LG, Sachs EM, Cima MJ. Mechanical properties of dense polylactic acid structures fabricated by three dimensional printing. *J Biomater Sci Polym Ed* 1996;8(1):63–75.
- [57] Sachlos E, Czernuszka J. Making tissue engineering scaffolds work review: the application of solid freeform fabrication technology to the production of tissue engineering scaffolds. *Eur Cell Mater* 2003;5:29–40.
- [58] Kim SS, Park MS, Jeon O, Choi CY, Kim BS. Poly(lactide–co-glycolide)/hydroxyapatite composite scaffolds for bone tissue engineering. *Biomaterials* 2006;27(8):1399–409.
- [59] Seitz H, Rieder W, Irsen S, Leukers B, Tille C. Three-dimensional printing of porous ceramic scaffolds for bone tissue engineering. *J Biomed Mater Res B Appl Biomater* 2005;74(2):782–8.
- [60] Bohner M. Calcium orthophosphates in medicine: from ceramics to calcium phosphate cements. *Injury* 2000;31(Suppl. 4):37–47.
- [61] Bohner M, Gbureck U, Barralet JE. Technological issues for the development of more efficient calcium phosphate bone cements: a critical assessment. *Biomaterials* 2005;26(33):6423–9.
- [62] Gbureck U, Holzel T, Doillon CJ, Muller FA, Barralet JE. Direct printing of bioceramic implants with spatially localized angiogenic factors. *Adv Mater* 2007;19(6):795.
- [63] Igawa K, Mochizuki M, Sugimori O, Shimizu K, Yamazawa K, Kawaguchi H, et al. Tailor-made tricalcium phosphate bone implant directly fabricated by a three-dimensional ink-jet printer. *J Artif Organs* 2006;9(4):234–40.
- [64] Mirtchi AA, Lemaitre J, Terao N. Calcium-phosphate cements–study of the beta-tricalcium phosphate–monocalcium phosphate system. *Biomaterials* 1989;10(7):475–80.
- [65] Kim S, Seong K, Kim O, Seo H, Lee M, Khang G, et al. Polyoxalate nanoparticles as a biodegradable and biocompatible drug delivery vehicle. *Biomacromolecules* 2010;11(3):555–60.
- [66] Alkhrasat MH, Marino FT, Retama JR, Jerez LB, Lopez-Cabarcos E. Beta-tricalcium phosphate release from brushite cement surface. *J Biomed Mater Res* 2008;84A(3):710–7.
- [67] Xu HHK, Carey LE, Simon CG, Takagi S, Chow LC. Premixed calcium phosphate cements: synthesis, physical properties, and cell cytotoxicity. *Dent Mater* 2007;23(4):433–41.
- [68] Tanaka S, Kishi T, Shimogoryo R, Matsuya S, Ishikawa K. Biopex acquires anti-washout properties by adding sodium alginate into its liquid phase. *Dent Mater* J 2003;22(3):301–12.
- [69] Suwanprateeb J, Sannang R, Suvannapruk W, Panyathanmaporn T. Mechanical and in vitro performance of apatite–wollastonite glass ceramic reinforced hydroxyapatite composite fabricated by 3D-printing. *J Mater Sci Mater Med* 2009;20(6):1281–9.
- [70] Kokubo T, Kim HM, Kawashita M. Novel bioactive materials with different mechanical properties. *Biomaterials* 2003;24(13):2161–75.
- [71] Gbureck U, Vorndran E, Muller FA, Barralet JE. “Low temperature direct 3D printed bioceramics and biocomposites as drug release matrices”. *J. Control Release* 2007;122(2):173–80.
- [72] Constantz BR, Ison IC, Fulmer MT, Poser RD, Smith ST, VanWagoner M, et al. Skeletal repair by in situ formation of the mineral phase of bone. *Science* 1995;267(5205):1796–9.
- [73] LeGeros RZ. Properties of osteoconductive biomaterials: calcium phosphates. *Clin Orthop Rel Res* 2002(395):81–98.
- [74] Dorozhkin SV, Epple M. Biological and medical significance of calcium phosphates. *Angew Chem Int Ed* 2002;41(17):3130–46.
- [75] White AA, Best SM, Kinloch IA. Hydroxyapatite–carbon nanotube composites for biomedical applications: a review. *Int J Appl Ceram Technol* 2007;4(1):1–13.
- [76] Burguera EF, Xu HHK, Takagi S, Chow LC. High early strength calcium phosphate bone cement: Effects of dicalcium phosphate dihydrate and absorbable fibers. *J Biomed Mater Res* 2005;75A(4):966–75.
- [77] Marra KG, Szem JW, Kumta PN, DiMilla PA, Weiss LE. In vitro analysis of biodegradable polymer blend/hydroxyapatite composites for bone tissue engineering. *J Biomed Mater Res* 1999;47(3):324–35.
- [78] Becker ST, Douglas T, Acil Y, Seitz H, Sivananthan S, Wiltfang J, et al. Biocompatibility of individually designed scaffolds with human periosteum for use in tissue engineering. *J Mater Sci Mater Med* 2010;21(4):1255–62.
- [79] Detsch R, Schaefer S, Deisinger U, Ziegler G, Seitz H, Leukers B. In vitro osteoclastic activity studies on surfaces of 3D printed calcium phosphate scaffolds. *J Biomater Appl* 2010 [Epub ahead of print].
- [80] Tamimi F, Torres J, Gbureck U, Lopez-Cabarcos E, Bassett DC, Alkhrasat MH, et al. Craniofacial vertical bone augmentation: a comparison between 3D printed monolithic monette blocks and autologous onlay grafts in the rabbit. *Biomaterials* 2009;30(31):6318–26.
- [81] Habibovic P, Gbureck U, Doillon CJ, Bassetta DC, van Blitterswijk CA, Barralet JE. Osteoconduction and osteoinduction of low-temperature 3D printed bioceramic implants. *Biomaterials* 2008;29(7):944–53.
- [82] Seitz H, Deisinger U, Leukers B, Detsch R, Ziegler G. Different calcium phosphate granules for 3-d printing of bone tissue engineering scaffolds. *Adv Eng Mater* 2009;11(5):B41–6.
- [83] Fierz FC, Beckmann F, Huser M, Irsen SH, Leukers B, Witte F, et al. The morphology of anisotropic 3D-printed hydroxyapatite scaffolds. *Biomaterials* 2008;29(28):3799–806.
- [84] Shanjani Y, De Croos JNA, Pilliar RM, Kandel RA, Toyserkani E. Solid freeform fabrication and characterization of porous calcium polyphosphate structures for tissue engineering purposes. *J Biomed Mater Res* 2010;93B(2):510–9.
- [85] Peters F, Groisman D, Davids R, Hanel T, Durr H, Klein M. Comparative study of patient individual implants from beta-tricalcium phosphate made by different techniques based on CT data. *Materialwiss Werkst* 2006;37(6):457–61.
- [86] Sun W, Darling A, Starly B, Nam J. Computer-aided tissue engineering: overview, scope and challenges. *Biotechnol Appl Biochem* 2004;39:29–47.
- [87] Sun W, Starly B, Darling A, Gomez C. Computer-aided tissue engineering: application to biomimetic modelling and design of tissue scaffolds. *Biotechnol Appl Biochem* 2004;39:49–58.
- [88] Polykandriotis E, Arkudas A, Euler S, Beier JP, Horch RE, Kneser U. Prevascularisation strategies in tissue engineering. *Handchir Mikrochir Plast Chir* 2006;38(4):217–23.
- [89] Barralet J, Gbureck U, Habibovic P, Vorndran E, Gerard C, Doillon CJ. Angiogenesis in calcium phosphate scaffolds by inorganic copper ion release. *Tissue Eng Part A* 2009;15(7):1601–9.
- [90] Jackson TR, Liu H, Patrikalakis NM, Sachs EM, Cima MJ. Modeling and designing functionally graded material components for fabrication with local composition control. *Mater Des* 1999;20(2–3):63–75.
- [91] Liu H, Maekawa T, Patrikalakis NM, Sachs EM, Cho W. Methods for feature-based design of heterogeneous solids. *Comput-Aided Des* 2004;36(12):1141–59.
- [92] Spillmann A. Flowability modification of lactose powder by plasma enhanced chemical vapor deposition. *Plasma Process Polym* 2007;4(1):S16–20.
- [93] Thurner PJ, Wyss P, Voide R, Stauber M, Stamparoni M, Sennhauser U, et al. Time-lapsed investigation of three-dimensional failure and damage accumulation in trabecular bone using synchrotron light. *Bone* 2006;39(2):289–99.
- [94] Nazarian A, Stauber M, Muller R. Design and implementation of a novel mechanical testing system for cellular solids. *J Biomed Mater Res Part B* 2005;73B(2):400–11.
- [95] Voide R, Van Lenthe GH, Schneider P, Thurner PJ, Wyss P, Sennhauser U, et al. 2006. Functional microimaging: An integrated approach for advanced bone biomechanics and failure analysis. *Progress in Biomedical Optics and Imaging Proceedings of SPIE*. 2006; 61431.
- [96] Holman RK, Cima MJ, Uhlend SA, Sachs E. Spreading and infiltration of inkjet-printed polymer solution droplets on a porous substrate. *J Colloid Interface Sci* 2002;249(2):432–40.
- [97] Tan KH, Chua CK, Leong KF, Naing MW, Cheah CM. Fabrication and characterization of three-dimensional poly(ether-ether-ketone)/hydroxyapatite biocomposite scaffolds using laser sintering. *Proc Inst Mech Eng Part H J Eng Med* 2005;219(3):183–94.
- [98] Williams JM, Adewunmi A, Schek RM, Flanagan CL, Krebsbach PH, Feinberg SE, et al. Bone tissue engineering using polycaprolactone scaffolds fabricated via selective laser sintering. *Biomaterials* 2005;26(23):4817–27.
- [99] Yang SF, Leong KF, Du ZH, Chua CK. The design of scaffolds for use in tissue engineering Part II. Rapid prototyping techniques. *Tissue Eng* 2002;8(1):1–11.
- [100] Choi JW, Wicker R, Lee SH, Choi KH, Ha CS, Chung I. Fabrication of 3D biocompatible/biodegradable micro-scaffolds using dynamic mask projection microstereolithography. *J Mater Proc Technol* 2009;209(15–16):5494–503.

- [101] Chu TMG, Halloran JW, Hollister SJ, Feinberg SE. Hydroxyapatite implants with designed internal architecture. *J Mater Sci Mater Med* 2001;12(6):471–8.
- [102] Heule M, Vuillemin S, Gauckler LJ. Powder-based ceramic meso- and microscale fabrication processes. *Adv Mater* 2003;15(15):1237–45.
- [103] Melchels FPW, Feijen J, Grijpma DW. A review on stereolithography and its applications in biomedical engineering. *Biomaterials* 2010;31(24):6121–30.
- [104] Michna S, Wu W, Lewis JA. Concentrated hydroxyapatite inks for direct-write assembly of 3-D periodic scaffolds. *Biomaterials* 2005;26(28):5632–9.
- [105] Miranda P, Pajares A, Guiberteau F. Finite element modeling as a tool for predicting the fracture behavior of robocast scaffolds. *Acta Biomater* 2008;4(6):1715–24.
- [106] Miranda P, Pajares A, Saiz E, Tomsia AP, Guiberteau F. Mechanical properties of calcium phosphate scaffolds fabricated by robocasting. *J Biomed Mater Res* 2008;85A(1):218–27.
- [107] Smay JE, Cesarano J, Lewis JA. Colloidal inks for directed assembly of 3-D periodic structures. *Langmuir* 2002;18(14):5429–37.
- [108] Miranda P, Saiz E, Gryn K, Tomsia AP. Sintering and robocasting of beta-tricalcium phosphate scaffolds for orthopaedic applications. *Acta Biomater* 2006;2(4):457–66.
- [109] Darling AL, Sun W. 3D microtomographic characterization of precision extruded poly-epsilon-caprolactone scaffolds. *J Biomed Mater Res Part B* 2004;70B(2):311–7.
- [110] Zein I, Hutmacher DW, Tan KC, Teoh SH. Fused deposition modeling of novel scaffold architectures for tissue engineering applications. *Biomaterials* 2002;23(4):1169–85.
- [111] Schantz JT, Brandwood A, Hutmacher DW, Khor HL, Bittner K. Osteogenic differentiation of mesenchymal progenitor cells in computer designed fibrin-polymer-ceramic scaffolds manufactured by fused deposition modeling. *J Mater Sci Mater Med* 2005;16(9):807–19.
- [112] Kalita SJ, Bose S, Hosick HL, Bandyopadhyay A. Development of controlled porosity polymer-ceramic composite scaffolds via fused deposition modeling. *Mater Sci Eng C Biomimetic Supramol Syst* 2003;23(5):611–20.
- [113] Wu BM, Borland SW, Giordano RA, Cima LG, Sachs EM, Cima MJ. Solid free-form fabrication of drug delivery devices. *J Control Release* 1996;40(1–2):77–87.
- [114] Park A, Wu B, Griffith LG. Integration of surface modification and 3D fabrication techniques to prepare patterned poly(L-lactide) substrates allowing regionally selective cell adhesion. *J Biomater Sci Polym Ed* 1998;9(2):89–110.
- [115] Suwanprateeb J, Chumnanklang R. Three-dimensional printing of porous polyethylene structure using water-based binders. *J Biomed Mater Res* 2006;78B(1):138–45.
- [116] Peters F, Hanel T, Bernhardt A, Lode A, Gelinsky M, Duerr H. 2008. In vitro examination of 3D printed vs. milled scaffolds from beta-tricalcium phosphate (beta-TCP) for patient individual bone regeneration. Postersession at the 8th World Biomaterials Congress, Amsterdam, Netherlands.
- [117] Bergmann C. 2008. Generative manufacturing of bone substitute implants made of a calciumphosphate-glass composite. Paper presented at the 10th International Symposium on Biomaterials: Fundamentals and Clinical Applications, Essen.
- [118] Szucs T, Brabazon D. 2007. Analysis of the effects of 3DP parameters on part feature dimensional accuracy. Paper presented at the Solid Freeform Fabrication (SFF) Symposium, Austin, TX.
- [119] Szucs T, Brabazon D. Effect of saturation and post processing on 3D printed calcium phosphate scaffolds. In: Prado M, Zavaglia C, editors. 21st International Symposium on Ceramics in Medicine. Buzios, Brazil; 2008. Available from: <http://www.scientific.net/KEM.396-398.663>.